

# Fluorescently labeled prey surrogates in combination with fluorescence-activated cell sorting successfully discriminate actively feeding mixotrophs in a lake water sample

Javier Florenza <sup>1\*,a</sup>, Anna-Maria Divne,<sup>2</sup> Stefan Bertilsson <sup>1,3</sup>

<sup>1</sup>Department of Ecology and Genetics, Uppsala University, Uppsala, Sweden

<sup>2</sup>Science for Life Laboratory, Department of Cell and Molecular Biology, Uppsala University, Uppsala, Sweden

<sup>3</sup>Department of Aquatic Sciences and Assessment, Swedish University of Agricultural Sciences, Uppsala, Sweden

## Abstract

Mixotrophic protists are capable of acting both as primary producers and primary consumers at the base of the aquatic food web, thus constituting key organisms in ecosystems where they are abundant. However, their identity, abundance, ecological dynamics, and biogeochemical impact in aquatic ecosystems remain understudied in comparison to classically demarcated autotrophs or heterotrophs. In this study, we make use of fluorescently labeled prey and fluorescence-activated cell sorting to taxonomically identify actively-feeding individual mixotrophic flagellates from lake water. Replicated experiments were carried out to assess the performance of three different fluorescently labeled prey types and a fluorescent dye targeting food vacuoles. In the experiments, water from an oligotrophic lake was exposed independently to each type of reporter and cells were individually sorted based on fluorescent signals for predation and chlorophyll *a*. A total of 927 individual single cells were successfully recovered, with all fluorescent reporters exhibiting high sensitivity for putative mixotrophic taxa: overall, 87% of the occurrences could be assigned to dictyochophytes, 9% to chrysophytes, and 3% to dinoflagellates. As a result, we were able to detect cryptic diversity within pedinellid algae and report a *Prorocentrum*-like freshwater occurrence. We argue that this procedure can be a valuable tool to uncover relevant and unexpected active mixotrophic species in a wider range of aquatic environments, and could easily be coupled to other techniques to describe the finer details of the trophic status of aquatic microbial communities.

Mixotrophy, defined as the combined capacity for photosynthesis and prey ingestion, is a widespread nutritional mode among aquatic planktonic protists, whether innate (constitutive mixotrophy, Sanders and Porter 1988) or acquired (Stoecker et al. 2009). Cases of acquired phototrophy by predatory phagotrophs are well documented in planktonic ciliates,

both in freshwaters and marine environments (Macek et al. 2006; Schoener and McManus 2012; Johnson and Beaudoin 2019), and in bloom-forming marine dinoflagellates (Carvalho et al. 2008). Constitutive mixotrophy is well established among freshwater chrysophytes (Bird and Kalf 1986; Sanders et al. 1990) and cryptophytes (Tranvik et al. 1989; Marshall and Laybourn-Parry 2002), and both freshwater and marine haptophytes (Jones et al. 1994; Granéli et al. 2012; Unrein et al. 2014) as well as dictyochophytes (Gerea et al. 2016; Li et al. 2021).

Nonetheless, novel cases of mixotrophy have recently been documented among marine raphidophytes (Jeong 2011), in an euglenozoan (Yamaguchi et al. 2012), a prasinophyte (Maruyama and Kim 2013), a chlorarachniophyte (Yoo and Palenik 2021) and, only from environmental samples, several bolidophytes (Frias-Lopez et al. 2009; Li et al. 2022). This, plus the proliferation of reports revealing unexpected mixotrophic behavior in taxa related to known mixotrophs (Jeong et al. 2005, within dinoflagellates; Yoo et al. 2017, within cryptophytes; Koppelle et al. 2022, within haptophytes) indicate that the

\*Correspondence: [xavi.florenza@ebc.uu.se](mailto:xavi.florenza@ebc.uu.se)

<sup>a</sup>Present address: Department of Organismal Biology, Uppsala University, Uppsala, Sweden

This is an open access article under the terms of the [Creative Commons Attribution](https://creativecommons.org/licenses/by/4.0/) License, which permits use, distribution and reproduction in any medium, provided the original work is properly cited.

Additional Supporting Information may be found in the online version of this article.

**Author Contribution Statement:** J.F. and S.B. designed the experiment and carried out field sampling. J.F., A.-M.D., and S.B. designed the cell sorting, amplification and sequencing library preparation strategies. J.F. and A.-M.D. performed cell sorting and A.-M.D. performed library preparation. J.F. analyzed the results and wrote the manuscript with contributions from A.-M.D. and S.B.

taxonomic spread of mixotrophy is broader than previously assumed, to the point that further exploration almost guarantees novelty (Li et al. 2022).

However, the mere presence of a taxon known to be capable of mixotrophy might not be sufficient to assess the mixotrophic status of the community at hand, since mixotrophy can be a very dynamic functional trait where functional potential will not necessarily reflect predation at any given time. This is exemplified by cryptophyte algae, which have been reported as active feeders (Tranvik et al. 1989; Marshall and Laybourn-Parry 2002) but also observed to rely exclusively on phototrophy even in presence of abundant prey (Isaksson et al. 1999; Blomqvist et al. 2001). Furthermore, mixotrophic assignments may be complicated when novel occurrences of mixotrophy are reported, such as the contended reports of mixotrophic activity in the green algae *Micromonas* spp. (Gonzalez et al. 1993; Sanders and Gast 2012; McKie-Krisberg and Sanders 2014), which is not mixotrophic (Wilken et al. 2019; Jimenez et al. 2021).

These instances underline the relevance of selectively identifying actively feeding mixotrophs from natural samples. Fluorescence-activated cell sorting (FACS) offers the potential to achieve this. Taking advantage of the combined fluorescence of chlorophyll *a* (Chl *a*), inherent to the mixotroph, with that of a reporter for prey ingestion, non-fixed actively feeding cells can be identified and isolated from a complex community sample in a high-throughput manner. After cell sorting and retrieval, a taxonomic marker can be amplified and sequenced to reveal the taxonomic identity of each single cell. Wilken et al. (2019) demonstrated the feasibility of the procedure when combining the specificity of food vacuole staining (Rose et al. 2004; Carvalho and Granéli 2006; Anderson et al. 2017) with Chl *a* autofluorescence.

In this study, we extend their approach and test the suitability and specificity of three different fluorescently labeled prey surrogates (fluorescently labeled tracers [FLT]), as reporters of microbial prey ingestion, to sort actively feeding mixotrophs from a natural sample in combination with chlorophyll fluorescence. We also included a food vacuole reporter, LysoSensor Blue DND-167, to compare FLT outcome to that of food vacuole staining.

## Materials and methods

A detailed account of the material and methods can be found in the Supporting Information “Extended Material and Methods” section.

### Sample collection and conditioning

The sample was collected on 15 October 2020 from oligotrophic, clear water lake Långsjön (60°1'58.5"N, 17°34'47.1"E,  $K_d = 0.52 \text{ m}^{-1}$ ). Water was retrieved from 1 m depth ( $T = 9^\circ\text{C}$ ) and filtered on-site through a nylon mesh (42  $\mu\text{m}$  cut-off size) into a clean collection bottle. Upon arrival to the laboratory (< 1 h from collection) 1 liter of the sample was transferred to a clean and autoclaved clear polystyrene bottle and left incubating at 18°C and a photon flux of approximately  $120 \mu\text{mol s}^{-1} \text{ m}^{-2}$  (measured with a spherical sensor, Biospherical Instruments QSL-100) under a 12-h photoperiod during 7 d. This was done to stimulate microeukaryote cell density in the sample so the experiment could be performed within a reasonable timeframe.

### Experimental set-up

To distinguish actively feeding mixotrophs from the rest of the community, the pre-incubated lake sample was exposed to four different feeding reporters in order to detect particle ingestion by chloroplast-bearing microeukaryotes: three of the reporters were based on the use of FLT and one additional reporter was based on food vacuole staining by LysoSensor™ Blue DND-167 (Invitrogen). Each of the FLT used in this experiment (Table 1) represented a different type class: inert (chemically inert Fluoresbrite® YG polystyrene microspheres—BDS—cat. no. 17154, Polysciences), dead (fluorescently labeled bacteria [FLB]-derived from heat-killed cultured *Escherichia coli* cells) and living (*E. coli* living cells expressing green fluorescent protein [GFP]). LysoSensor (LYS) is an acidotropic molecule that fluoresces when protonated ( $\text{pK}_a = 5.1$ ) and has successfully been used to track food vacuoles by feeding microeukaryotes (Carvalho and Granéli 2006). For each of the prey reporters, small volumes of FLT suspensions (10–15  $\mu\text{L}$ ) were added to 20 mL fractions of the sample to a final density of  $1.1\text{--}1.5 \cdot 10^5 \text{ FLT mL}^{-1}$ , and each fraction was incubated at 18°C during 40 min in the absence of light. After that time, 5 mL of each incubation were fixed with an equal volume of freshly prepared, ice-cold 4% formaldehyde in phosphate buffer saline (PBS, incl. 0.85% NaCl, adjusted to  $\text{pH} \approx 7.5$ ) and 5 mL were

**Table 1.** FLT used in this study.

Tracer	Description	Volume ( $\mu\text{m}^3$ )	Quality class
BDS	Polystyrene microspheres, 0.98 $\mu\text{m}$	0.49 (CV 9%) <sup>a</sup>	Inert
FLB	Fluorescently labeled <i>Escherichia coli</i> cells	0.76 (CV 41%)	Dead
GFP	<i>E. coli</i> TOP10 pQE30-tGFP	0.72 (CV 48%)	Living

<sup>a</sup>Based on 3% CV in diameter values declared by the manufacturer.

placed on ice and taken to the sorter in the shortest possible time. Ice treatment was necessary to arrest feeding behavior during sample transportation to the sorter without compromising its cytometric detection (see Florenza and Bertilsson 2023 for further details on ice treatment). The fixed fraction was meant to be further examined under the microscope to confirm FLT ingestion within the double-positive (chlorophyll fluorescence and either FLT or LYS fluorescence) cytometric population. For the food vacuole reporter, 20 mL fractions of the sample were kept at 18°C in the absence of light during 30 min, after which LYS was added (0.5  $\mu$ M final concentration) and incubated 10 additional min before placing 5 mL in ice prior to sorting. All treatments were performed in triplicate. In addition, one 20 mL fraction with no supplement of neither FLT nor LYS was kept during 40 min under the same experimental conditions (18°C, no light) and taken to the sorter to be used as negative control to establish the sorting gates. To profile the taxonomic composition of the sample at the time of the experiment, three 50 mL fractions were filtered onto 0.2  $\mu$ m pore size, 25 mm in diameter polycarbonate (PC) membrane filters which were subsequently frozen until DNA extraction.

### Single-cell sorting

Cell sorting was performed with a MoFlo Astrios EQ (Beckman Coulter) on 384 well plates. Sorting decisions were based on the concomitant signal of chlorophyll autofluorescence and either FLT or food vacuole fluorescence (double positives). The three prey types were detected using red vs green fluorescence (640–671/30 height log vs. 488–530/40 height log). Food vacuole staining was detected by red vs. blue fluorescence (640–671/30 height log or 355–448/59 height log). For each sorting experiment, double-positive single individual cells were directly deposited into 2  $\mu$ L of lysis buffer (0.5% Triton X-100 in 0.1 M Tris-HCl buffer). Plates were frozen and kept at –80°C until further processing. To confirm mixotrophy in the FACS double-positive population, 100 cells from the fixed fractions of the 3 different prey reporters were sorted in bulk onto no. 1 glass coverslips for microscopy to confirm particle ingestion. The slides were examined at 1000 $\times$  total magnification with a Nikon Eclipse E600 epifluorescence microscope (Nikon) by simultaneously detecting FLT and chlorophyll fluorescence (B-2A filter set, Nikon).

### Lysis and whole genome amplification of sorted single cells

Single cells in lysis buffer were thawed and incubated at 95°C for 1 min and briefly cooled down on ice before multiple displacement amplification (MDA). MDA reactions were run at 30°C for 6–7 h in 10  $\mu$ L volume and were monitored in real time by detection of SYTO13 fluorescence. The single amplified genomes (SAGs) were stored at –20°C until further processing. All the sequenced DNA originating from this collection of isolates is from here on referred to as the single-cell dataset.

### DNA extraction from PC filters

DNA from biological material deposited onto filter surfaces was extracted using the DNeasy PowerSoil Pro kit (Qiagen), placing one filter per tube and following the manufacturer's instructions. All the amplified and sequenced DNA originating from this extract is from here on referred to as the total community dataset.

### Amplicon generation, library preparation, and Illumina sequencing

#### Single-cell dataset

Diluted SAGs (30–40 $\times$ ) from the four different treatments were run in 10  $\mu$ L polymerase chain reactions (PCRs) targeting the V4–V5 regions of the 18S rRNA gene. The 574\*f forward and 1132r reverse primers were chosen to maximize the recoverable taxonomic breadth (Hugerth et al. 2014). To accomplish the level of intended multiplexing capacity using only 384 commercially available indices, the target-specific PCR1 primers were designed to have a 5-bp barcode specific for each of the 4 treatments. This design enabled pooling of single-cell reactions from the different replicated treatments prior (4-cell minipools) to the index PCR to create a maximum of 4  $\times$  384 barcoded combinations. Detailed barcode and primer sequences can be found in Supporting Information Table S1. Single-cell minipools were prepared for sequencing with IDT Illumina Nextera™ DNA Unique Dual (UD) index sets A–D (Illumina) for unique dual indexing and further multiplexing. The final pool was sequenced using Illumina MiSeq v3 PE 2  $\times$  300 bp including a 10% Phi-X spike-in.

#### Total community dataset

A total of 6  $\mu$ L of each extract were run in triplicate in 20  $\mu$ L PCRs using modified 574\*f and 1132r primers, in this case excluding the barcode sequence. Products of PCR1 triplicates were pooled and purified using the Monarch DNA cleanup kit (New England Biolabs) according to the manufacturer's instructions. Index PCRs were carried out in 20  $\mu$ L reactions using the IDT Illumina Nextera™ DNA UD index set A for combinatorial indexing and sample multiplexing. Triplicate amplicon libraries were added to a bigger pool and sequenced using Illumina MiSeq v3 PE 2  $\times$  300 bp including a 5% Phi-X spike-in.

### Read processing and annotation

#### Single-cell dataset

Raw sequences were demultiplexed based on Nextera UD indexes, then quality filtered and further demultiplexed based on treatment barcode by imposing matching barcodes on both members of each pair. High-quality, fully demultiplexed reads, distributed across 933 samples, were denoised using the DADA2 algorithm (Callahan et al. 2016). Resulting amplicon sequence variants (ASVs) were annotated using the classifier implemented in DADA2. The PR2 Reference Sequence Database version 4.14.0 (Guillou et al. 2013) was used as reference

for assigning taxonomy. Taxonomic annotation was considered satisfactory when bootstrap support was 80 or higher at genus level. Abundant variants that did not meet this requirement were annotated based on small subunit (SSU) rRNA gene phylogenies (see below). To remove amplification noise, low-abundance ASVs which were co-occurrent and highly similar to other abundant ASVs were filtered out using LULU (Frøslev et al. 2017) and clustered into operational taxonomic units (OTUs) at 97% sequence similarity using VSEARCH (Rognes et al. 2016). The details and rationale for this procedure can be found in the Supporting Information “Extended Material and Methods” section.

### Total community dataset

Raw sequences were quality filtered by cropping the reads at the first uncalled position, if present (default behavior in DADA2), then retaining reads longer than 275 bp, and were further denoised into ASVs. All steps were carried out within the DADA2 R package. ASVs were clustered to 97% similarity and annotated analogously to the single-cell dataset.

### SSU rRNA gene phylogenies

The Ochrophyta SSU rRNA gene multiple sequence alignment (MSA) was built and manually curated based on unique, high quality publicly available sequences (see Extended Extended Materials and Methods for alignment details). The final MSA consisted of 371 sequences, including the 18 OTUs under scrutiny. Sequence identifiers and accession numbers can be found in Supporting Information Table S2. All phylogenies were constructed using RAxML version 8 (Stamatakis 2014) implementing the GTR substitution model combined with the CAT approximation of rate heterogeneity, invoking a rapid bootstrap search (100 replicates) followed by a thorough ML search on the given alignment.

### Statistical analyses

The DESeq2 R package implementation of a generalized linear model based on the negative binomial distribution (Love et al. 2014) was used to evaluate differences in the taxonomic counts generated by each treatment. To visualize differences in output among treatments, principal component analysis (PCA) based on a regularized log<sub>2</sub> transformation of the count data (implemented within the DESeq2 package) was performed. For the analysis of method specificity, false-positive relative frequencies ( $\hat{fp}$ ) were calculated for each replicate as the ratio between the number of potential false positives  $FP$  and the total number of occurrences:

$$\hat{fp} = \frac{FP}{n} \quad (1)$$

and were averaged per treatment ( $\widehat{fp}$ ). Statistical support for differences among treatments was obtained by estimating 95% confidence intervals on bootstrapped pairwise ratios

(1000 bootstraps, Efron and Tibshirani 1994) of integrated false-positive frequencies ( $\widehat{\theta}_{ij}$ ):

$$\widehat{\theta}_{ij} = \frac{FP_i/N_i}{FP_j/N_j} \quad (2)$$

where  $FP_i$  is the total number of potential false positives across all replicates for treatment  $i$ ,  $FP_j$  its equivalent for treatment  $j$ ,  $N_i$  is the total sample size across all replicates for treatment  $i$  and  $N_j$  its equivalent for treatment  $j$ .  $FP$  was tallied according to two different scenarios: under the most exclusive scenario, all cases where mixotrophy could not be unambiguously established were considered false positives; under the most inclusive scenario, all these cases were considered true positives. The actual frequency of false positives for each treatment is assumed to lie in between.

## Results

### Taxonomic composition of the dataset

For our experiments, we FACS-sorted 1837 single events of which 961 were successfully amplified into a sequencing library (see Supporting Information Table S3 for the full account per experiment and replicate). Upon sequencing and after read quality filtration, 6.4 million paired short reads were obtained, yielding a median 4676 reads per sorted event (see Supporting Information Fig. S1 for frequency distributions of number of reads per sample). Reads were denoised, filtered based on sequence similarity and co-occurrence patterns across isolates, further clustered at 97% identity, and taxonomically annotated and curated to yield 34 high-quality OTUs (annotation of all isolates is collected in Supporting Information Table S4). We could successfully annotate 927 of all sorted events, of which 99% were identified as belonging to either the Dictyochophyceae, Chrysophyceae, Dinophyceae, Cryptophyceae or Prymnesiophyceae (Fig. 1A; Table 2). All these groups include well documented examples of mixotrophic lifestyles.

Dictyochophyceae vastly dominated the dataset, followed at great distance by Chrysophyceae and Dinophyceae (Table 2). Together, representatives of these classes added up to 938 occurrences, making up for slightly more than 97% of the total occurrences in the dataset. Three Cryptophyceae and two Prymnesiophyceae completed the cases of potential mixotrophic flagellates recovered from the sample. The remaining fraction of the dataset (< 2%) was composed of anecdotal occurrences of taxa that are known to be unpigmented (Supporting Information Table S5). These most likely represent heterotrophic organisms that were physically associated with a chlorophyll-bearing cell and responded somehow to our ingestion tracers (e.g., having ingested both FLT and pigmented prey). Since these taxa are known to be incapable of photosynthesis, they were not considered to be true mixotrophs and thus represented false positives of the methodology.



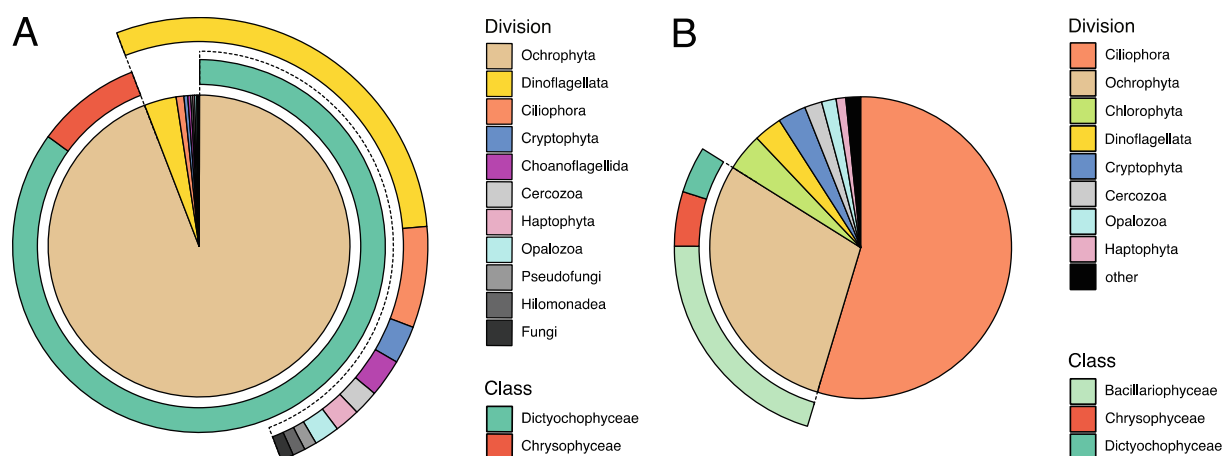


**Fig. 1.** Relative abundance of taxa represented in the single-cell scoring positive for both Chl *a* fluorescence and prey ingestion (A) and the total community (B) datasets. The relative proportions shown in the plots are built according to the number of sorted single cells (A) or the total number of reads (B) recovered per taxon. Taxonomic annotation at division and class levels follows PR2 taxonomy (Guillou et al. 2013).

Dictyochophyceae occurrences could be microscopically characterized as mixotrophic. Chloroplast arrangements typical of pedinellid dictyochophytes (Sekiguchi et al. 2003) were confirmed upon microscopic examination of fixed cells that had been FACS-sorted in identical fashion as the rest of the sample (Fig. 2; Supporting Information Fig. S2). To further refine sequence identity within the pedinellids for all sorted OTUs, SSU rRNA gene phylogenies spanning the entire Ochrophyta phylum (and therefore comprising the Dictyochophyceae) were constructed, including all ochrophyte OTUs recovered in the single-cell dataset (Fig. 3). The phylogeny identified OTU\_2 as being closely related to two *Pseudopedinella* strains with very short branches and high bootstrap support, suggesting that this variant could represent a species resembling the *Pseudopedinella* genus. In addition, four OTUs formed two phylogenetically strong groups of sequences (OTU\_1 with OTU\_170, and OTU\_11 with OTU\_29), which may represent two members from the same genus. These pairs, together with the remaining

dictyochophyte OTUs, showed enough phylogenetic signal to be placed within pedinellids but were sufficiently divergent to any known SSU rRNA pedinellid sequence. Therefore, these OTUs represent molecular novelty within mixotrophic pedinellids.

The second most abundant group represented in the single-cell dataset are the Chrysophyceae. In contrast to the Dictyochophyceae, none of the cells observed in the FACS-mediated microscopy preparations could be unequivocally identified as a chrysophyte, and thus microscopic support of feeding and pigmentation could not be obtained for this group. However, multiple independent events of pigmentation loss are well characterized throughout the chrysophyte phylogeny (Dorrell et al. 2019), and many cases of non-photosynthetic, leucoplast-bearing chrysophytes have been described (e.g., *Paraphysomonas* spp. or *Spumella* spp.; Lim et al. 1999; Boenigk et al. 2005; Grossmann et al. 2016). Accordingly, finer phylogenetic annotation was necessary to

**Table 2.** Putatively mixotrophic occurrences in the single-cell dataset, their frequency and their number of associated OTUs. Singlet refers to a sorted event associated to a single OTU whereas doublet refers to an event where two different OTUs co-occur, in both cases after read filtering and manual curation after taxonomic annotation (see “Materials and methods” section).

Class	Number of occurrences			Fraction of the total* (%)	Number of OTUs
	Total	Singlets	Doublets		
Dictyochophyceae	817	783	34†	84.9	9
Chrysophyceae	88	84	4‡	9.1	9
Dinophyceae	33	5	28§	3.4	1
Cryptophyceae	3	3	0	0.3	2
Prymnesiophyceae	2	2	0	0.2	1
Total	943	877	66	98.1	22

\*Considering a total of 961 taxonomic occurrences distributed across 927 single sorted events (893 singlets and 34 doublets).

†Of these, 2 occurrences are paired with another dictyochophyte, 2 with a chrysophyte, and 27 with a dinoflagellate.

‡Of these, two occurrences are paired with a dictyochophyte and two with a dinoflagellate.

§Of these, 27 occurrences are paired with a dictyochophyte and 2 with a chrysophyte.

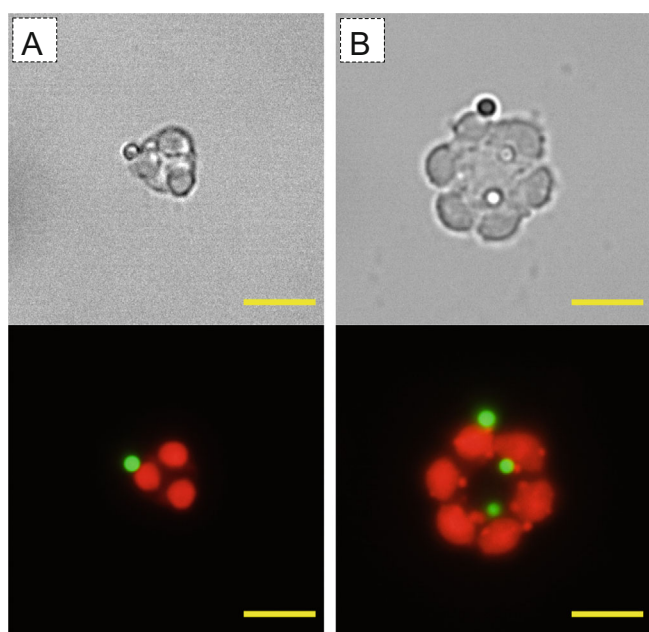


**Fig. 2.** The two pedinellid morphotypes observed in the study. Upper pictures: phase contrast. Lower pictures: epifluorescence micrographs showing the chloroplasts in red and ingested 1- $\mu$ m fluorescent microspheres in green. Scale bar: 10  $\mu$ m.

ascertain the mixotrophic nature of the retrieved chrysophyte OTUs. The full Ochrophyte SSU rRNA gene phylogeny showed that the chrysophyte occurrences in the sorted cells, although accounting only for 9% of the total dataset, were very diverse and spread throughout the class (Fig. 3). However, the difficulty of assigning pigmentation to our sorted chrysophyte occurrences was apparent in the tree: of all the OTUs, only 4 (OTU\_3, OTU\_23, OTU\_27 and OTU\_65) could be determined as non-pigmented with confidence, while the pigmentation of the rest remained uncertain to varying degrees. Consequently, their identity as putative mixotrophs, although likely, cannot be attributed with certainty. This was taken into account when the specificity of each capture approach was analyzed (see below).

The third most abundant putative mixotrophic group is represented by a single OTU (OTU\_16, Table 2) annotated as *Prorocentrum* sp. based on sequence similarity (> 80% bootstrap support). Interestingly, 85% (28 out of 33) of all putative *Prorocentrum* occurrences were associated to a dictyochophyte OTU (i.e., they formed doublets in a single sorting event, Table 2). This high rate of co-occurrence could be explained by *Prorocentrum* sp. feeding on the abundant pedinellids (Fig. 1B), each doublet reflecting an occasion in which either an FLT-fed pedinellid was recently ingested by the dinoflagellate or where the dinoflagellate had ingested both FLT and the pedinellid. We considered these scenarios to be plausible given the reported *Prorocentrum* spp. strong preference for algal prey (Jeong et al. 2005; Johnson 2015). Therefore, since the ultimate predator in such association would be *Prorocentrum* sp., its doublets were considered as Dinophyceae singlets

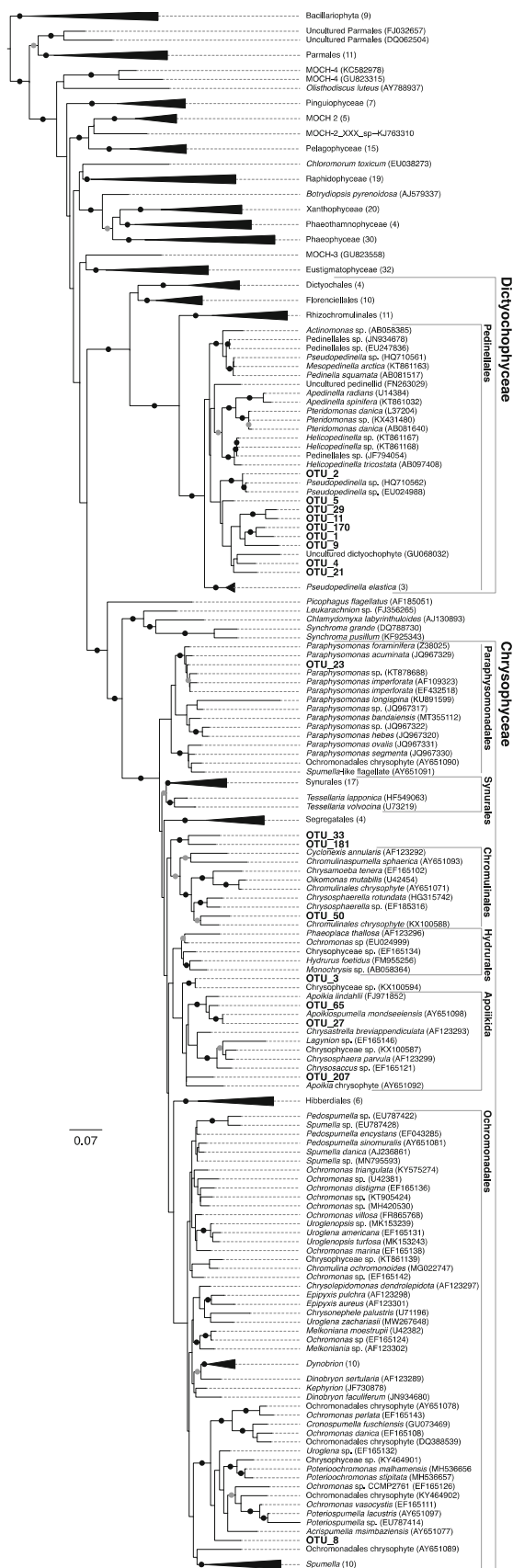
when comparing the output of each of the methodologies employed (see “Amplicon generation, library preparation, and Illumina sequencing,” “Read processing and annotation,” and “SSU rRNA gene phylogenies” sections).

Finally, three cryptophyte (OTU\_47 twice and OTU\_240 once) and two prymnesiophyte occurrences (both OTU\_53) completed the taxa that accounted for putative mixotrophs captured with the method. Based on sequence similarity over PR2 sequences, OTU\_47 was identified as *Cryptomonas curvata* (100% bootstrap support), while OTU\_240 could only be annotated with confidence to the order level (Cryptomonadales). While some cryptophytes have been seen capable of phagotrophy (Tranvik et al. 1989; Urabe et al. 2000; Marshall and Laybourn-Parry 2002), the phagotrophic potential in some species might be lost or not manifested (Isaksson et al. 1999; Blomqvist et al. 2001). Hence, the cryptophyte OTUs are considered to be of uncertain feeding behavior when comparing tracer performance. OTU\_53 was annotated as *Chrysochromulina parva* based on sequence similarity (100% bootstrap support), and thus affiliation to at least the genus was given as certain. *Chrysochromulina* spp. are known to be mixotrophic algae (Jones et al. 1994).

### Comparison to sample background

SSU rRNA amplicon sequencing of the sample background produced 88,100 reads that were quality filtered, denoised, and clustered at 97% nucleotide identity to yield 368 OTUs. The total community dataset was greatly dominated by ciliates and diatoms, which together accounted for almost 75% of the reads (Fig. 1B). The ciliate group was diverse (Oligohymenophorea, 0.4%; Litostomatea, 1.7%; Prostomatea, 3%; Spirotrichea, 19; and *Askenasia* sp., 27%). Diatoms were dominated by the genus *Stephanodiscus*, which accounted for almost 19% of the total read count in the sample.

Putatively mixotrophic classes accounted for 18.6% of the reads in the dataset. These included, in descending order of abundance, chrysophytes (8%), dictyochophytes (5%), cryptophytes (2.8%), dinoflagellates (2.8%), and prymnesiophytes (1%). Therefore, at class level, no putatively mixotrophic group was found in the total community beyond those identified in the sorted cells. At sequence level, only a few putatively mixotrophic variants were recovered in the total community (5 dictyochophyte variants and 11 chrysophyte variants, Supporting Information Figs. S3, S4) that were not represented in the 932 isolates. These could represent either colorless taxa belonging to those clades, mixotrophic algae not suitable for cell sorting (e.g., colonial forms) or not feeding at the time of sampling, or simply very scarce taxa (the median relative abundances for those variants are < 0.01%). Such cases are further explored in the discussion section. Inversely, almost all OTUs represented in the isolate dataset were represented by sequences in the total community dataset (Supporting Information Table S6), with OTU\_240 as the sole exception



with a single occurrence. Since each dataset had been generated independently, we thus find strong support that OTUs associated to sorted cells corresponded to cells that were originally present in the sample.

### Effect of fluorescent reporter in taxa recovery

To test whether incubation with FLT types of different quality could lead to differences in mixotrophic taxa recovery, incubations with three different FLT types (fluorescent polystyrene microspheres, heat-killed fluorescently labeled *E. coli* cells and living GFP-expressing *E. coli* cells, referred to as BDS, FLB, and GFP tracers, respectively) were replicated three times. In addition, three replicates based on food vacuole staining with acidotropic stain LysoSensor Blue DND-167 (LYS reporter, Carvalho and Granéli 2006) were also performed.

Based on the relative frequencies of recovered taxa at class level, the main differences in output were seen between the LYS reporter and all the FLT-based treatments, where all the latter gave similar results (Fig. 4). In general, LYS differed from all the other reporters by delivering a lower proportion of OTUs of non-dicochyophyte origin. FLTs tended to deliver a higher proportion of chrysophytes (10–11% on average for each FLT, vs. 4% for LYS) and of *Prorocentrum* sp. (4–5% vs. 1%). Further differences were observed in the proportion of non-mixotrophic OTUs, where bacteria-based tracers (FLB and GFP) returned 4%, whereas they represented 1% of the total occurrences for both BDS and LYS reporters. Only BDS and GFP returned multiplets (i.e., doublets, 2 and 3 respectively).

FACS-sorting cytograms of all sorted events (Fig. 5) showed that the distribution of chrysophyte occurrences was skewed toward lower values of chlorophyll fluorescence. The effect was most obvious in Fig. 5B,C, where many chrysophytes were located very close to the lower chlorophyll intensity threshold (see Supporting Information Fig. S5 for sorting gates and gating strategy, and Supporting Information Table S3 for ratios of sorted events over total events recorded above the chlorophyll intensity threshold).

Signs of predator preference were also seen within dicochyophytes when comparing the relative abundance of dicochyophyte OTUs among reporters (Supporting Information Fig. S5). Clear examples of these were OTU\_2 (*Pseudopedinella* sp.), which was overrepresented when sorting based on microspheres (BDS); OTU\_11, overrepresented when

**Fig. 3.** Phylogenetic tree of the 18S rRNA gene spanning the entire Ochrophyta phylum with Bacillariophyta as the outgroup. Gray dots indicate 75–90% bipartition bootstrap support, while black dots indicate support above 90%. OTUs captured in this experiment are highlighted in bold letters. GenBank accession numbers are included in parenthesis. For collapsed taxa, the number in parenthesis indicates the amount of sequences that conform the group. The length of the polygon corresponds to that of the longest branch of the collapsed subtree. Complete sequence identity and GenBank accession numbers for all sequences can be found in Supporting Information Table S2.

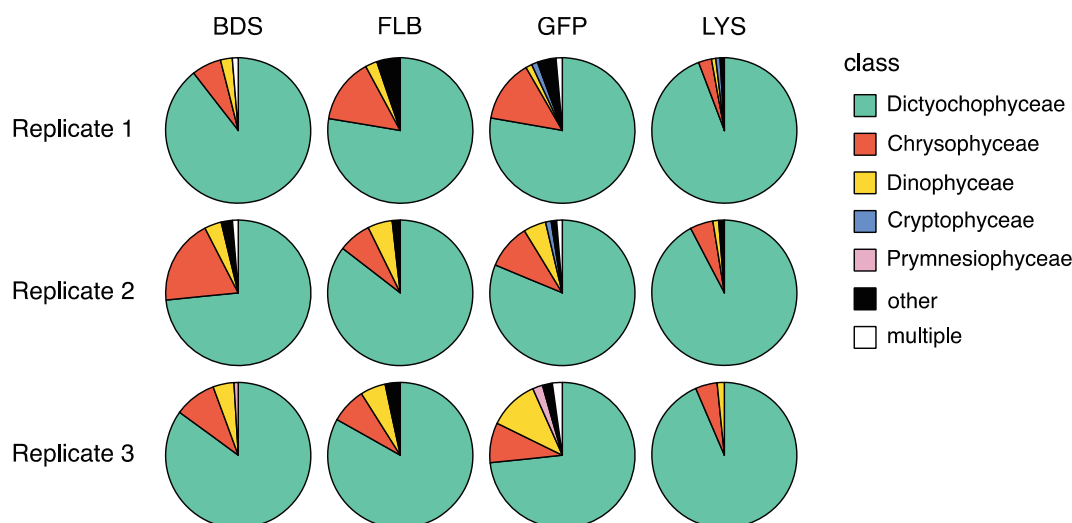


**Fig. 4.** Pie charts showing the relative frequency of taxa recovered, at class, level, per fluorescent reporter and replicate. Reporters: 1  $\mu\text{m}$  fluorescent microspheres (BDS), FLB from *Escherichia coli* cells (FLB), GFP-expressing *E. coli* cells (GFP) and food vacuole staining with LysoSensor Blue DND-167 (LYS).

sorting based on living prey (GFP); and OTU\_29, almost absent of any of the FLT treatments (recovered with LysoSensor staining in 12 out of 14 total occurrences). These findings point to cryptic ecological differentiation among closely related pedinellids which merits further study.

#### Differential abundance analysis

To obtain further support for differences across reporters, a differential abundance analysis of recovered taxa per reporter was performed. For that purpose, a set of features were defined at two levels, either taxonomic classes at broad level or OTUs at fine level, and their abundances were modeled according to the generalized linear model implementation in the DESeq2 R package (Love et al. 2014).

At broad scale, significant differences (at 95% confidence or lower) in taxon abundance were only found between the LYS reporter and all the other tracers (illustrated in Fig. 6A). This difference was driven exclusively by the dictyochophyte occurrences, for which LYS was significantly enriched. This confirms what could be intuitively observed based on relative abundances in Fig. 4.

At a finer scale, differences among reporters driven by OTU identity became more apparent, allowing the identification of three reporter groups in the PCA space (Fig. 6B). Again, differences were mainly driven by dictyochophyte OTUs (which was expected, since they were by far the most abundant occurrences), and partially confirmed what can be seen in Supporting Information Fig. S5: the BDS tracer significantly enriched for OTU\_2 compared to any other reporter, and OTU\_29 abundance was significantly higher in cells retrieved using the LYS reporter. However, no significant differences in output could be seen for the two bacterial tracers (FLB and GFP, grouped together along PC1), despite the apparent slight preference of OTU\_11 for living prey. Overall, all OTUs that

were recovered more than 5 times by any reporter were also recovered by all the other reporters, with the only exception of OTU\_29, which is recovered 12 times by LYS, 2 by GFP, and is absent from both BDS and FLB.

In general, differential abundances between treatments was most apparent at class level when considering the choice in the approach (either prey-based tracers or food vacuole staining), while the choice of prey surrogate (microspheres vs. bacterial types) influenced the outcome at higher resolution (e.g., OTU level). In any case, differences among reporters were not critical for taxa recovery.

#### Mixotroph specificity

As discussed above, recovered OTUs known to lack pigmentation represent false positives. In turn, pigmented OTUs which spuriously appear as feeding would also account as such. Since five of the recovered chrysophyte OTUs are of unsure pigmentation (see above) and cryptophyte feeding behavior remains uncertain, false positives delivered by each reporter were tallied based on two scenarios: one in which all such OTUs were considered non-mixotrophic (most exclusive scenario), and one in which they were all considered to be mixotrophic (most inclusive scenario). The underlying relative frequency of false positives (i.e., the number of false positives divided by the number of occurrences, Eq. 1 in “Statistical analyses” section) was accordingly considered to lie somewhere in between.

Regardless of scenario, the relative frequency of false positives averaged across replicates ( $\hat{f}_p$ ) delivered by the LYS reporter was significantly lower than that of any other reporter (Fig. 7; Supporting Information Fig. S6). In addition, no significant differences were found in  $\hat{f}_p$  among FLT-based approaches. The  $\hat{f}_p$  for FLTs was found to lie, on average, between 14% and 10% (for most exclusive and most inclusive scenario, respectively), while LYS  $\hat{f}_p$  was between 5% and 3%.



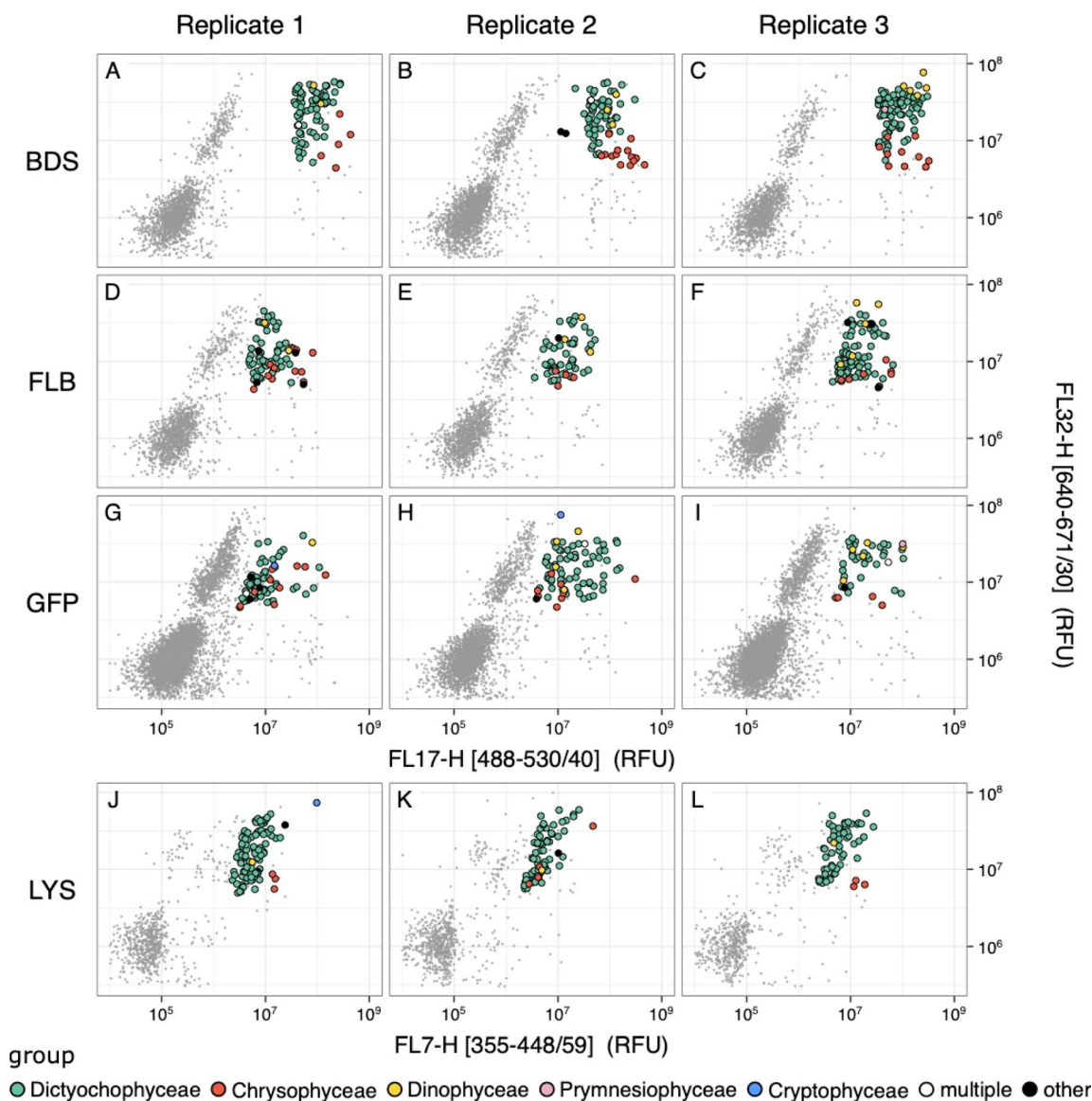


**Fig. 5.** FACS-sorting cytograms showing all the sorted single cells when color-coded based on their taxonomic annotation at class level. Multiple occurrences (in white) refer to doublets not involving OTU\_16 (Dinophyceae). Gray dots represent a subsample of events of the background population. Gates and gating strategy to discriminate the mixotrophic population are found in Supporting Information Fig. S5. FL7, blue fluorescence following UV excitation; FL17, green fluorescence following blue light excitation; FL32, red fluorescence following red light excitation. FL7 corresponds to food vacuole fluorescence, FL17 to FLP fluorescence and FL32 to chlorophyll fluorescence. RFU, relative fluorescence units. Reporters are letter-coded as in Fig. 4.

Moreover, the larger spread of  $\hat{fp}$  associated to the use of FLTs denoted their higher susceptibility to false positives. LYS, in contrast, delivered consistent results across replicates. Altogether, we found that LysoSensor Blue was more specific, robust and consistent than any prey-based reporter.

**Discussion**

In this study, we demonstrate that the combined signals of a fluorescent proxy for prey ingestion and intrinsic chlorophyll autofluorescence can provide high specificity for

successful FACS-mediated recovery of individual actively feeding mixotrophs from aquatic samples. Due to the single-cell resolution and flow cytometry nature of the approach, we are able to associate the taxonomic identity of a large number of sorted cells to their fluorescent mixotrophic signature and decipher the robustness of the mixotroph retrieval.

Consequently, this strategy represents a valuable alternative to uncover mixotrophic diversity and more broadly describe microeukaryote novelty at genomic, taxonomic and ecological levels. Nevertheless, the method is not devoid of certain constraints and limitations, and therefore the outcome

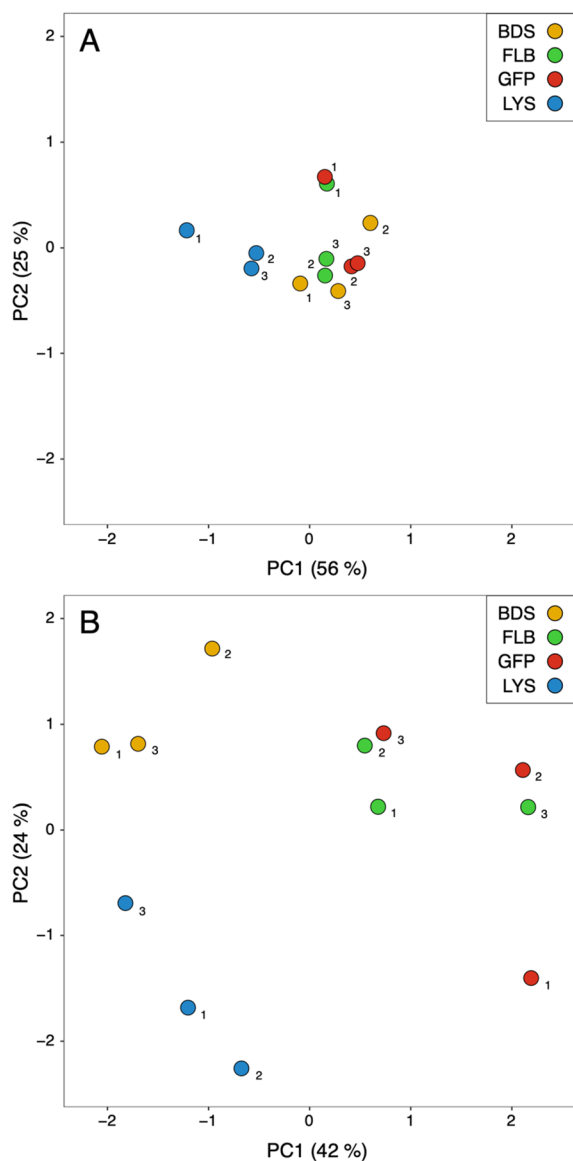


**Fig. 6.** PCA plots of regularized log-transformed count matrices of taxonomic occurrences across reporter and replicate at class level (A) and OTU level (B). Numbers next to each dot indicate the corresponding replicate. Reporters: 1  $\mu$ m fluorescent microspheres (BDS, yellow dots), FLB from *Escherichia coli* cells (FLB, green dots), GFP-expressing *E. coli* cells (GFP, red dots) and food vacuole staining with LysoSensor Blue DND-167 (LYS, blue dots).

should be interpreted with care. The approach is based on the critical assumption that chlorophyll and concomitant reporter fluorescence are a unique indication of mixotrophy, but that might not be the case. Other phenomena of biological nature might obscure the output of the methodology, such as mutualistic interactions between a pigmented cell and an opportunistic predatory host (see Stoecker et al. 2009 for a well-documented collection of cases), multispecies successions of kleptoplastidy (Anschütz et al. 2022) or ingestion events in which a colorless predator feeds indistinctively on autotrophic and heterotrophic prey. In such instances, food vacuole or

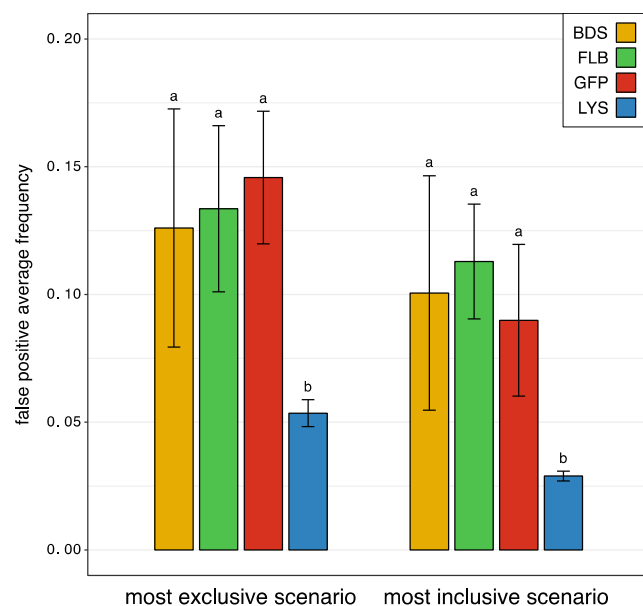


**Fig. 7.** Barplots showing false-positive average frequency per reporter when calculated considering ambiguous occurrences as non-mixotrophic (most exclusive scenario) or mixotrophic (most inclusive scenario). Error bars represent the standard error of the mean. Lettered notation above bars designates significantly different groups resulting from the estimation of 95% confidence intervals from bootstrapped pairwise false-positive ratios ( $\hat{\theta}_{ij}$ , Eq. 2 in “Materials and Methods” section). Reporters: 1  $\mu$ m fluorescent microspheres (BDS), FLB from *E. coli* cells (FLB), GFP-expressing *E. coli* cells (GFP) and food vacuole staining with LysoSensor Blue DND-167 (LYS).

FLT fluorescence could coexist inside the same cell without it being an indication of mixotrophy. This is well exemplified by many of the occurrences collected in Table S5, but also by the uncertainty around the chrysophyte occurrences. The evolutionary incidence of pigmentation loss is in fact also high in other ecologically important mixotrophic groups such as the dictyochophytes or cryptophytes, and colorless members of both have been shown to be avid bacterial grazers (Sleigh and Zubkov 1998; Grujic et al. 2018). This limiting factor is thus prevalent within mixotrophic groups and could be inherent to their mixotrophic nature, since it may be costly in evolutionary terms to maintain the potential for parallel heterotrophic and autotrophic nutrition (Raven 1997; Stoecker 1998). Microscopic evidence of phagotrophy within sorted cells might therefore be fundamental to validate claims of mixotrophy in novel OTUs (Wilken et al. 2019).

Finally, the association of a particular microeukaryote to FLT fluorescence might not indicate phagotrophy with absolute certainty. Diverse physiological states of phytoplankton cells, independent of phagocytosis, might involve the excretion of polysaccharides that can confer stickiness to the cell surface (Seymour et al. 2017). In this scenario, FLTs might attach to non-feeding cells and therefore generate non-phagocytic associations between cells and FLTs. For example, Wilken et al. 2019 showed that cultures of non-phagocytotic

*Micromonas polaris* displayed low but increasing associations to FLT with increasing time in absence of light, and attributed increased cell stickiness to cell senescence. The impact of such an issue is difficult to predict, but can arguably be expected to be small: the incidence of such cases within the FLT-positive, chlorophyll-positive population would be low when true mixotrophs are present. If that is the case, non-phagocytotic associations to FLT would be represented in low numbers in the final dataset. Therefore, caution is warranted when interpreting the feeding lifestyle of doubtful instances when recovered in low frequencies.

Despite the possible influence of these obscuring factors, we could show that the specificity of the methodology for mixotrophic eukaryotes is high with worst-case occurrences of false positives below 15% for all the reporters explored in our study. Quantitatively, the frequency of all potentially obscuring cases can therefore be expected to be low and thus their impact small when actual mixotrophic taxa are present in the sample.

#### Technical shortcomings of the methodology

Even when a FACS instrument is at hand, which might in itself be a decisive constraint, the particle size that can be precisely sorted and isolated in a such an instrument has a relatively low upper threshold. Typically, the maximum sortable cell size dimension is recommended to be about one third of the diameter of the sorting nozzle, and thus restriction in particle size is indispensable for an analysis like the one reported here. In our case, the size cut-off applied in our experiment was 40  $\mu\text{m}$  (for a nozzle of 100  $\mu\text{m}$  in diameter), effectively excluding larger objects from our analyses. This necessary threshold could, however, lead to overlooking larger ecologically important microeukaryotes, such as free-living mixotrophic oligotrich ciliates (Stoecker et al. 2009; Agatha and Strüder-Kypke 2014) or colony-forming mixotrophic chrysophytes like *Dinobryon* sp. or *Uroglena* sp. (Bird and Kalff 1986) known to be voracious bacterivores.

Once the cells are sorted, failure to lyse single cells can also influence mixotroph underrepresentation in the resulting dataset. Due to more or less elaborate structures encasing the cells (green algae cellulose walls, dinoflagellate thecas, diatom frustules, coccolith or organic scales in haptophytes, periplast in cryptophytes, etc.), some cell morphologies will be inherently harder to lyse than others. No universal lysis method exists that is fully compatible with downstream enzymatic reactions (Brown and Audet 2008; Lynn and Pinheiro 2009; Woyke et al. 2017) necessary to amplify a taxonomic marker of a single cell. In our experiments, 50% of the sorted events failed to reach annotation, in most cases due to failure to amplify the SSU rRNA gene. Whether this phenomenon is driven by poor lysis efficiency alone is difficult to judge, since the direct evaluation of single-cell lysis in microwells is not practical. Nevertheless, failure to access the DNA of some of the sorted events might indeed cause taxa to remain hidden.

#### Differences brought by the type of reporter

The choice of feeding reporter might itself introduce biases in mixotroph recovery. Predator preference for certain FLT is unavoidable (Landry et al. 1991; Boenigk et al. 2001; Anderson et al. 2017), while acidotropic probes have gathered some concern about their specificity (Rose et al. 2004; Wilken et al. 2019). Unavoidably, differences in the taxonomic profile that result from the use of different reporters for prey ingestion are expected. As an example, overrepresentation of chrysophytes when using FLT compared to their recovery seen when using LysoSensor could be explained by differing predator preference for surrogate prey. In this case, chrysophyte affinity for big sized prey (which has been shown in the past for *Ochromonas* strains, e.g., Chrzanowski and Šimek 1990, Florenza and Bertilsson 2023) might be higher to that of dictyochophytes, increasing the proportion of the former over the latter when using FLT. If so, this phenomenon would not occur when using food vacuole treatment, because the relative proportion of dictyochophytes to chrysophytes would not be affected by FLT preference. Since many of the chrysophytes reported represent false positives, LYS treatment, under this scenario, might be driving slightly lower false-positive recovery in our experiment.

Nevertheless, taking our investigation as a reference, the variability introduced by the type of reporter employed seems to be rather minor. Figures 4 and 6 show, when interpreted jointly, that overall differences among reporters seen in our dataset were driven by only a few taxa. The clearest divide was observed between the strategy based on food vacuole staining and those based on FLT and is driven by a reduced proportion of OTUs associated with the methodological constraints outlined above. Some minor differences were observed between the bacteria-based types (FLB and GFP) and the synthetic FLT type (i.e., fluorescence microspheres), which seemed to be differentially preferred by OTU\_2. No significant differences were observed between bacterial prey types, suggesting that the quality of being dead or alive has little impact in the identity of recovered taxa. Finally, most recurring taxa were to some extent recovered by all reporters. Thus, in general, differences among treatments, although consistent, appeared to be minor. Therefore, we conclude and suggest that the impact of the reporter is of secondary importance when the goal is to identify actively feeding mixotrophs in a sample, but caution should still be taken when interpreting results quantitatively.

#### On food vacuole staining

Regardless of outcome, food vacuole staining delivers greater performance to FLT treatment in terms of capture efficiency, since it targets all feeding cells in the population, whereas only a fraction of these will have ingested a FLT at any given moment. As a consequence, faster sorting rates can be achieved which, in turn, allow deeper screening of the sample per unit time. However, caution is advised when using this kind of dyes since not only food vacuoles, but also other

acidic organelles, are susceptible to be stained (*see* any of the works just referenced). Hence, the potential risk associated to such probes when used as reporter for ingestion is a higher yield of false positives. To probe this assumption, food vacuole staining was included in the overall comparison because attempts to retrieve actively feeding mixotrophs from aquatic samples based on such tracers have already been published (Wilken et al. 2019). Hence, a comparison between the performance of the FLT-based approach and that based on food vacuole staining was deemed to be of interest.

In our experiments, the use of LysoSensor Blue DND-167 is not associated to a higher false-positive rate, but rather accounted for the lowest false-positive rates among all reporters tested. We speculate that the specific use of LysoSensor Blue DND-167, rather than acidotropic probes in general, might be responsible for this high specificity. For instance, (Wilken et al. 2019) use the combined fluorescent signals of chlorophyll and the acidotropic LysoSensor Yellow/Blue DND-160 to target mixotrophs in marine samples in a way analogous to our study. In this study they reported on the recovery of diatoms, non-mixotrophic and thus spurious, using this dye. However, LysoSensor Yellow/Blue DND-160 is known to specifically stain silicon deposition vesicles (SDVs) in diatoms (Shimizu et al. 2001). In contrast, to our knowledge, no such conflicting affinity has been reported for LysoSensor Blue DND-167, and in agreement with this we do not recover any diatom OTU in our single-cell dataset despite their high abundance in the total community (Fig. 1B).

Another common dye, LysoTracker Green DND-26, has been used successfully as a tracer for ingestion (Sintes and del Giorgio 2010; Martinez-Garcia et al. 2012), but nonetheless shown spurious green fluorescence from photosynthetic, non-phagotrophic *Micromonas pusilla* (albeit at very low intensities when compared to heterotrophs, Rose et al. 2004) and non-specific fluorescence in *Dinophysis norvegica* (Carvalho and Granéli 2006). Furthermore, (Wilken et al. 2019) report the same issue with diatom SDVs observed for LysoSensor Yellow/Blue. Carvalho and Granéli (2006), however, did indeed report food vacuole specificity for LysoSensor Blue in their study.

Combined, these results suggest that the food-vacuole specificity of LysoSensor Blue could be superior to that of LysoSensor Yellow/Blue and LysoTracker probes. We acknowledge, nonetheless, that LysoSensor Blue could still pose some limitations that might not have been apparent in our study. Given the obvious advantages of tracing ingestion based on acidotropic probes (illustrated in this study and in all references mentioned in the last paragraphs), a cross comparison between the three dyes commented here, on a varied number of organisms and combining cytometric and microscopic evidence, would be valuable for gaining conclusive evidence in this matter.

A final advantage in the use of LysoSensor Blue over LysoSensor Yellow/Blue or LysoTracker Green is its compatibility with the use of fluorescein-stained FLTs like those

employed in our study. A three-color sorting strategy (LysoSensor Blue, FLT and Chl *a*) could achieve enhanced specificity for mixotrophy, since one ingestion reporter would contribute to rule out the spurious cases associated to the other. While it would affect sorting performance (delivering low sorting efficiencies typical of FLT reporters), it would maximize the confidence in the assignment of feeding mode. Hence, this would represent the most robust implementation of the approach, provided that microeukaryote density is not a severe limitation in the sample.

Overall, we demonstrate quantitatively that FACS-based sorting of double positives for Chl *a* and an ingestion reporter is a methodology capable of recovering actively feeding mixotrophs from an environmental sample. As a result, we are able to uncover cryptic diversity within pedinellid algae and report a *Prorocentrum*-like freshwater occurrence. We therefore believe this procedure represents a valuable tool to detect relevant and unexpected active mixotrophic species in a wider range of aquatic environments, and could easily be coupled to other techniques to describe the finer details of the trophic status of aquatic microbial communities.

### Data availability statement

All sequencing data generated for this study have been deposited in the European Nucleotide Archive (ENA) at EMBL-EBI under accession number PRJEB55831. All cytometric data, including metadata linking cytometric information to sequencing output, are available at FlowRepository, International Society for the Advancement of Cytometry, under experiment ID FR-FCM-Z6AT.

### References

- Agatha, S., and M. C. Strüder-Kypke. 2014. What morphology and molecules tell us about the evolution of Oligotrichea (Alveolata, Ciliophora). *Acta Protozool.* **53**: 77–90.
- Anderson, R., K. Jürgens, and P. J. Hansen. 2017. Mixotrophic phytoflagellate bacterivory field measurements strongly biased by standard approaches: A case study. *Front. Microbiol.* **8**: 1–12.
- Anschütz, A. A., K. J. Flynn, and A. Mitra. 2022. Acquired phototrophy and its implications for bloom dynamics of the *Teleaulax-Mesodinium-Dinophysis*-complex. *Front. Mar. Sci.* **8**: 1–18.
- Bird, D. F., and J. Kalff. 1986. Bacterial grazing by planktonic lake algae. *Science* **231**: 493–496.
- Blomqvist, P., M. Jansson, S. Drakare, A. K. Bergström, and L. Brydsten. 2001. Effects of additions of DOC on pelagic biota in a clearwater system: Results from a whole lake experiment in northern Sweden. *Microb. Ecol.* **42**: 383–394.
- Boenigk, J., C. Matz, K. Jürgens, and H. Arndt. 2001. The influence of preculture conditions and food quality on the ingestion and digestion process of three species of



- heterotrophic nanoflagellates. *Microb. Ecol.* **42**: 168–176.
- Boenigk, J., K. Pfandl, P. Stadler, and A. Chatzinotas. 2005. High diversity of the “*Spumella*-like” flagellates: An investigation based on the SSU rRNA gene sequences of isolates from habitats located in six different geographic regions. *Environ. Microbiol.* **7**: 685–697.
- Brown, R. B., and J. Audet. 2008. Current techniques for single-cell lysis. *J. R. Soc. Interface* **5**: S131–S138.
- Callahan, B. J., P. J. McMurdie, M. J. Rosen, A. W. Han, A. J. A. Johnson, and S. P. Holmes. 2016. DADA2: High-resolution sample inference from Illumina amplicon data. *Nat. Methods* **13**: 581–583.
- Carvalho, W. F., and E. Granéli. 2006. Acidotropic probes and flow cytometry: A powerful combination for detecting phagotrophy in mixotrophic and heterotrophic protists. *Aquat. Microb. Ecol.* **44**: 85–96.
- Carvalho, W. F., S. Minnhagen, and E. Granéli. 2008. *Dinophysis norvegica* (Dinophyceae), more a predator than a producer? *Harmful Algae* **7**: 174–183.
- Chrzanowski, T. H., and K. Šimek. 1990. Prey-size selection by freshwater flagellated protozoa. *Limnol. Oceanogr.* **35**: 1429–1436.
- Dorrell, R. G., and others. 2019. Principles of plastid reductive evolution illuminated by nonphotosynthetic chrysophytes. *Proc. Natl. Acad. Sci. USA* **116**: 6914–6923.
- Efron, B., and R. J. Tibshirani. 1994. An introduction to the bootstrap. Chapman & Hall.
- Florenza, J., and S. Bertilsson. 2023. Choice of methodology and surrogate prey are decisive for the quality of protistan bacterivory rate estimates. *Aquat. Microb. Ecol.* **89**: 43–53.
- Frias-Lopez, J., A. Thompson, J. Waldbauer, and S. W. Chisholm. 2009. Use of stable isotope-labelled cells to identify active grazers of picocyanobacteria in ocean surface waters. *Environ. Microbiol.* **11**: 512–525.
- Frøslev, T. G., R. Kjøller, H. H. Bruun, R. Ejrnaes, A. K. Brunbjerg, C. Pietroni, and A. J. Hansen. 2017. Algorithm for post-clustering curation of DNA amplicon data yields reliable biodiversity estimates. *Nat. Commun.* **8**: 1188.
- Gerea, M., J. F. Saad, I. Izaguirre, C. Queimaliños, J. M. Gasol, and F. Unrein. 2016. Presence, abundance and bacterivory of the mixotrophic algae *Pseudopedinella* (Dictyochophyceae) in freshwater environments. *Aquat. Microb. Ecol.* **76**: 219–232.
- Gonzalez, J. M., B. F. Sherr, and E. B. Sherr. 1993. Digestive enzyme activity as a quantitative measure of protistan grazing: The acid lysozyme assay for bacterivory. *Mar. Ecol. Prog.* **100**: 197–206.
- Granéli, E., B. Edvardsen, D. L. Roelke, and J. A. Hagström. 2012. The ecophysiology and bloom dynamics of *Prymnesium* spp. *Harmful Algae* **14**: 260–270.
- Grossmann, L., C. Bock, M. Schweikert, and J. Boenigk. 2016. Small but manifold—Hidden diversity in “*Spumella*-like flagellates”. *J. Eukaryot. Microbiol.* **63**: 419–439.
- Grujicic, V., J. K. Nuy, M. M. Salcher, T. Shabarova, V. Kasalicky, J. Boenigk, M. Jensen, and K. Šimek. 2018. Cryptophyta as major bacterivores in freshwater summer plankton. *ISME J.* **12**: 1668–1681.
- Guillou, L., and others. 2013. The protist ribosomal reference database (PR2): A catalog of unicellular eukaryote small sub-unit rRNA sequences with curated taxonomy. *Nucleic Acids Res.* **41**: 597–604.
- Hugerth, L. W., E. E. L. Muller, Y. O. O. Hu, L. A. M. Lebrun, H. Roume, D. Lundin, P. Wilmes, and A. F. Andersson. 2014. Systematic design of 18S rRNA gene primers for determining eukaryotic diversity in microbial consortia. *PLoS One* **9**: e95567.
- Isaksson, A., A. K. Bergström, P. Blomqvist, and M. Jansson. 1999. Bacterial grazing by phagotrophic phytoflagellates in a deep humic lake in northern Sweden. *J. Plankton Res.* **21**: 247–268.
- Jeong, H. J. 2011. Mixotrophy in red tide algae raphidophytes. *Eukaryot. Microbiol.* **58**: 215–222.
- Jeong, H. J., Y. D. Yoo, J. Y. Park, J. Y. Song, S. T. Kim, S. H. Lee, K. Y. Kim, and W. H. Yih. 2005. Feeding by phototrophic red-tide dinoflagellates: Five species newly revealed and six species previously known to be mixotrophic. *Aquat. Microb. Ecol.* **40**: 133–150.
- Jimenez, V., J. A. Burns, F. le Gall, F. Not, and D. Vaultot. 2021. No evidence of phago-mixotrophy in *Micromonas polaris* (Mamiellophyceae), the dominant picophytoplankton species in the Arctic. *J. Phycol.* **57**: 435–446.
- Johnson, M. D. 2015. Inducible mixotrophy in the dinoflagellate *Prorocentrum minimum*. *J. Eukaryot. Microbiol.* **62**: 431–443.
- Johnson, M. D., and D. J. Beaudoin. 2019. The genetic diversity of plastids associated with mixotrophic oligotrich ciliates. *Limnol. Oceanogr.* **64**: 2187–2201.
- Jones, H. L. J., B. S. C. Leadbeater, and J. C. Green. 1994. Mixotrophy in haptophytes, p. 247–263. *In* J. C. Green and B. S. C. Leadbeater [eds.], *The haptophyte algae*. Clarendon Press.
- Koppelle, S., and others. 2022. Mixotrophy in the bloom-forming genus *Phaeocystis* and other haptophytes. *Harmful Algae* **17**: 102292.
- Landry, M. R., J. M. Lehner-Fournier, J. A. Sundstrom, V. L. Fagerness, and K. E. Selph. 1991. Discrimination between living and heat-killed prey by a marine zooflagellate, *Paraphysomonas vestita* (Stokes). *J. Exp. Mar. Biol. Ecol.* **146**: 139–151.
- Li, Q., K. F. Edwards, C. R. Schvarcz, K. E. Selph, and G. F. Steward. 2021. Plasticity in the grazing ecophysiology of *Florenciella* (Dictyochophyceae), a mixotrophic nanoflagellate that consumes *Prochlorococcus* and other bacteria. *Limnol. Oceanogr.* **66**: 47–60.
- Li, Q., K. F. Edwards, C. R. Schvarcz, and G. F. Steward. 2022. Broad phylogenetic and functional diversity among

- mixotrophic consumers of *Prochlorococcus*. *ISME J.* **16**: 1557–1569.
- Lim, E. L., M. R. Dennett, and D. A. Caron. 1999. The ecology of *Paraphysomonas imperforata* based on studies employing oligonucleotide probe identification in coastal water samples and enrichment cultures. *Limnol. Oceanogr.* **44**: 37–51.
- Love, M. I., W. Huber, and S. Anders. 2014. Moderated estimation of fold change and dispersion for RNA-seq data with DESeq2. *Genome Biol.* **15**: 1–21.
- Lynn, D. H., and M. Pinheiro. 2009. A survey of polymerase chain reaction (PCR) amplification studies of unicellular protists using single-cell PCR. *J. Eukaryot. Microbiol.* **56**: 406–412.
- Macek, M., C. Callieri, K. Šimek, and A. L. Vázquez. 2006. Seasonal dynamics, composition and feeding patterns of ciliate assemblages in oligotrophic lakes covering a wide pH range. *Arch. Hydrobiol.* **166**: 261–287.
- Marshall, W., and J. Laybourn-Parry. 2002. The balance between photosynthesis and grazing in Antarctic mixotrophic cryptophytes during summer. *Freshw. Biol.* **47**: 2060–2070.
- Martinez-Garcia, M., D. Brazel, N. J. Poulton, B. K. Swan, M. L. Gomez, D. Masland, M. E. Sieracki, and R. Stepanauskas. 2012. Unveiling in situ interactions between marine protists and bacteria through single cell sequencing. *ISME J.* **6**: 703–707.
- Maruyama, S., and E. Kim. 2013. A modern descendant of early green algal phagotrophs. *Curr. Biol.* **23**: 1081–1084.
- McKie-Krisberg, Z. M., and R. W. Sanders. 2014. Phagotrophy by the picoeukaryotic green alga *Micromonas*: Implications for Arctic Oceans. *ISME J.* **8**: 1953–1961.
- Raven, J. A. 1997. Phagotrophy in phototrophs. *Limnol. Oceanogr.* **42**: 198–205.
- Rognes, T., T. Flouri, B. Nichols, C. Quince, and F. Mahé. 2016. VSEARCH: A versatile open source tool for metagenomics. *PeerJ* **10**: 1–22.
- Rose, J. M., D. A. Caron, M. E. Sieracki, and N. Poulton. 2004. Counting heterotrophic nanoplanktonic protists in cultures and aquatic communities by flow cytometry. *Aquat. Microb. Ecol.* **34**: 263–277.
- Sanders, R. W., and K. G. Porter. 1988. Phagotrophic phytoflagellates, p. 167–192. *In* K. Marshall [ed.], *Advances in microbial ecology*. Springer.
- Sanders, R. W., K. G. Porter, and D. A. Caron. 1990. Relationship between phototrophy and phagotrophy in the mixotrophic chrysophyte *Poterioochromonas malhamensis*. *Microb. Ecol.* **19**: 97–109.
- Sanders, R. W., and R. J. Gast. 2012. Bacterivory by phototrophic picoplankton and nanoplankton in Arctic waters. *FEMS Microbiol. Ecol.* **82**: 242–253.
- Schoener, D. M., and G. B. McManus. 2012. Plastid retention, use, and replacement in a kleptoplastidic ciliate. *Aquat. Microb. Ecol.* **67**: 177–187.
- Sekiguchi, H., M. Kawachi, T. Nakayama, and I. Inouye. 2003. A taxonomic re-evaluation of the Pedinellales (Dictyochophyceae), based on morphological, behavioural and molecular data. *Phycologia* **42**: 165–182.
- Seymour, J. R., S. A. Amin, J. B. Raina, and R. Stocker. 2017. Zooming in on the phycosphere: The ecological interface for phytoplankton-bacteria relationships. *Nat. Microbiol.* **2**: 17065.
- Shimizu, K., Y. del Amo, M. A. Brzezinski, G. D. Stucky, and D. E. Morse. 2001. A novel fluorescent silica tracer for biological silicification studies. *Chem. Biol.* **8**: 1051–1060.
- Sintes, E., and P. A. del Giorgio. 2010. Community heterogeneity and single-cell digestive activity of estuarine heterotrophic nanoflagellates assessed using lysotracker and flow cytometry. *Environ. Microbiol.* **12**: 1913–1925.
- Sleigh, M. A., and M. V. Zubkov. 1998. Methods of estimating bacterivory by protozoa. *Eur. J. Protistol.* **34**: 273–280.
- Stamatakis, A. 2014. RAxML version 8: A tool for phylogenetic analysis and post-analysis of large phylogenies. *Bioinformatics* **30**: 1312–1313.
- Stoecker, D. K. 1998. Conceptual models of mixotrophy in planktonic protists and some ecological and evolutionary implications. *Eur. J. Protistol.* **34**: 281–290.
- Stoecker, D. K., M. D. Johnson, C. De Vargas, and F. Not. 2009. Acquired phototrophy in aquatic protists. *Aquat. Microb. Ecol.* **57**: 279–310.
- Tranvik, L. J., K. G. Porter, and J. M. Sieburth. 1989. Occurrence of bacterivory in *Cryptomonas*, a common freshwater phytoplankton. *Oecologia* **78**: 473–476.
- Unrein, F., J. M. Gasol, F. Not, I. Forn, and R. Massana. 2014. Mixotrophic haptophytes are key bacterial grazers in oligotrophic coastal waters. *ISME J.* **8**: 164–176.
- Urabe, J., T. B. Gurung, T. Yoshida, T. Sekino, M. Nakanishi, M. Maruo, and E. Nakayama. 2000. Diel changes in phagotrophy by *Cryptomonas* in Lake Biwa. *Limnol. Oceanogr.* **45**: 1558–1563.
- Wilken, S., C. C. M. Yung, M. Hamilton, K. Hoadley, J. Nzongo, C. Eckmann, M. Corrochano-Luque, C. Poirier, and A. Z. Worden. 2019. The need to account for cell biology in characterizing predatory mixotrophs in aquatic environments. *Philos. Trans. R. Soc. B Biol. Sci.* **374**: 20190090.
- Woyke, T., D. F. R. Doud, and F. Schulz. 2017. The trajectory of microbial single-cell sequencing. *Nat. Methods* **14**: 1045–1054.
- Yamaguchi, A., N. Yubuki, and B. S. Leander. 2012. Morphostasis in a novel eukaryote illuminates the evolutionary transition from phagotrophy to phototrophy: Description of *Rapaza viridis* n. gen. et sp. (Euglenozoa, Euglenida). *BMC Evol. Biol.* **12**: 29.
- Yoo, Y. D., and hv. 2017. Mixotrophy in the marine red-tide cryptophyte *Teleaulax amphioxieia* and ingestion and grazing impact of cryptophytes on natural populations of bacteria in Korean coastal waters. *Harmful Algae* **68**: 105–117.
- Yoo, Y. D., and B. Palenik. 2021. Growth and grazing of the chlorarachniophyte *Bigelowiella natans* (Chlorarachniophyceae) on the marine cyanobacterium *Synechococcus*. *Phycologia* **60**: 375–383.

## Acknowledgments

This work was financed by the EU's Horizon 2020 research and innovation program under the Marie Skłodowska-Curie ITN project SINGEK (grant agreement no. H2020-MSCA-ITN-2015-675752), by FORMAS (project 2022-01211), and by Malménska Studiestiftelsen grant awarded to J.F. J.F. would like to thank P. Leroy (Swedish University of Agricultural Sciences) for providing the transformed *E. coli* strain used in this study, and M. Jamy, M. Méndez Sandín, and F. Burki for their valuable insights in building and interpreting the phylogenies. The authors would like to acknowledge support from the Genomics infrastructure services at Science for Life Laboratory. Single-cell sorting, whole genome amplification and amplicon library preparation were performed at the Microbial Single Cell Genomics Facility (MSCG), to which this investigation is much indebted. The work reported here would have hardly been possible without their open-ended, microbe-driven disposition. Sequencing was performed by the SNP&SEQ Technology Platform. Both facilities are part of the Uppsala node at the National Genomics Infrastructure (NGI) Sweden and Science

for Life Laboratory. The SNP&SEQ Platform is also supported by the Swedish Research Council and the Knut and Alice Wallenberg Foundation. Data analysis was enabled by the resources provided by the Swedish National Infrastructure for Computing (SNIC) at Uppsala University, partially funded by the Swedish Research Council through grant agreement no. 2018-05973.

## Conflict of Interest

The authors declare no conflict of interest.

*Submitted 05 May 2023*

*Revised 15 December 2023*

*Accepted 23 February 2024*

*Associate editor: Maren Striebel*